

1

2

3

4

5

6

## **Supplementary Information**

7

### **Plasmon-enhanced Stimulated Raman Scattering Microscopy with**

8

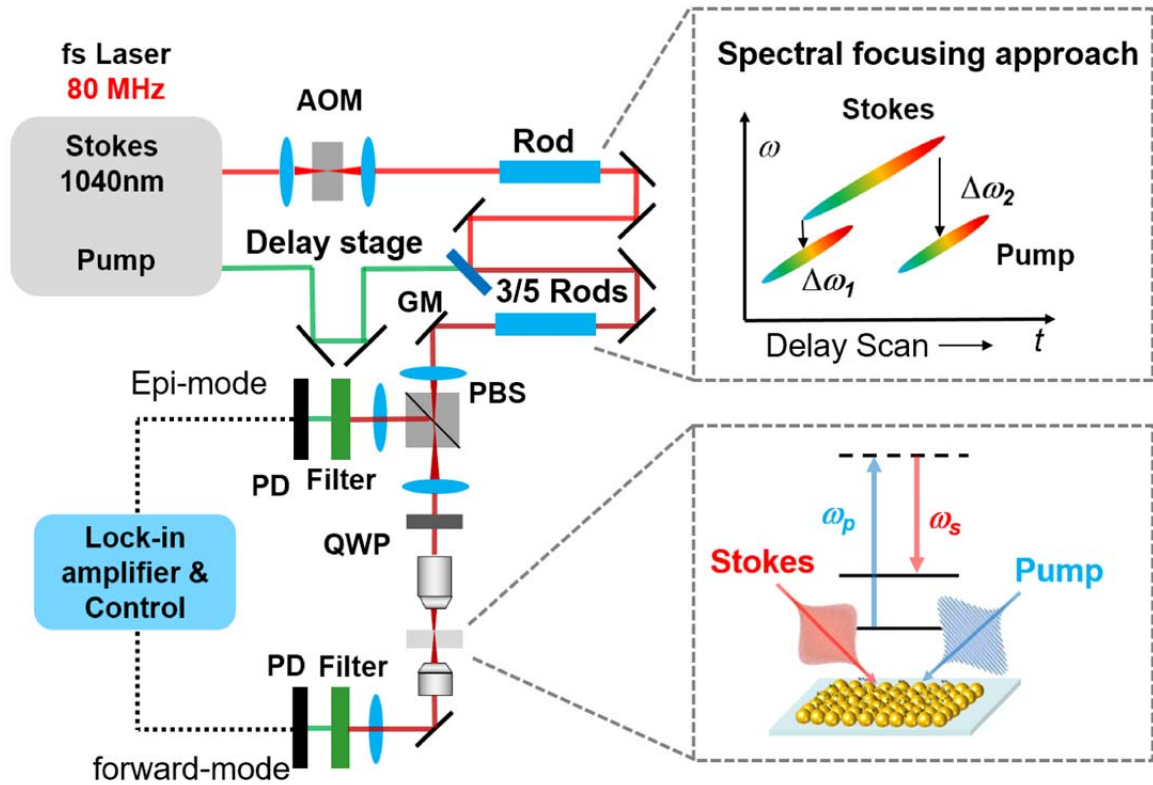
### **Single-molecule Detection Sensitivity**

9

Cheng Zong et al.

10

11 **Supplementary Figure**

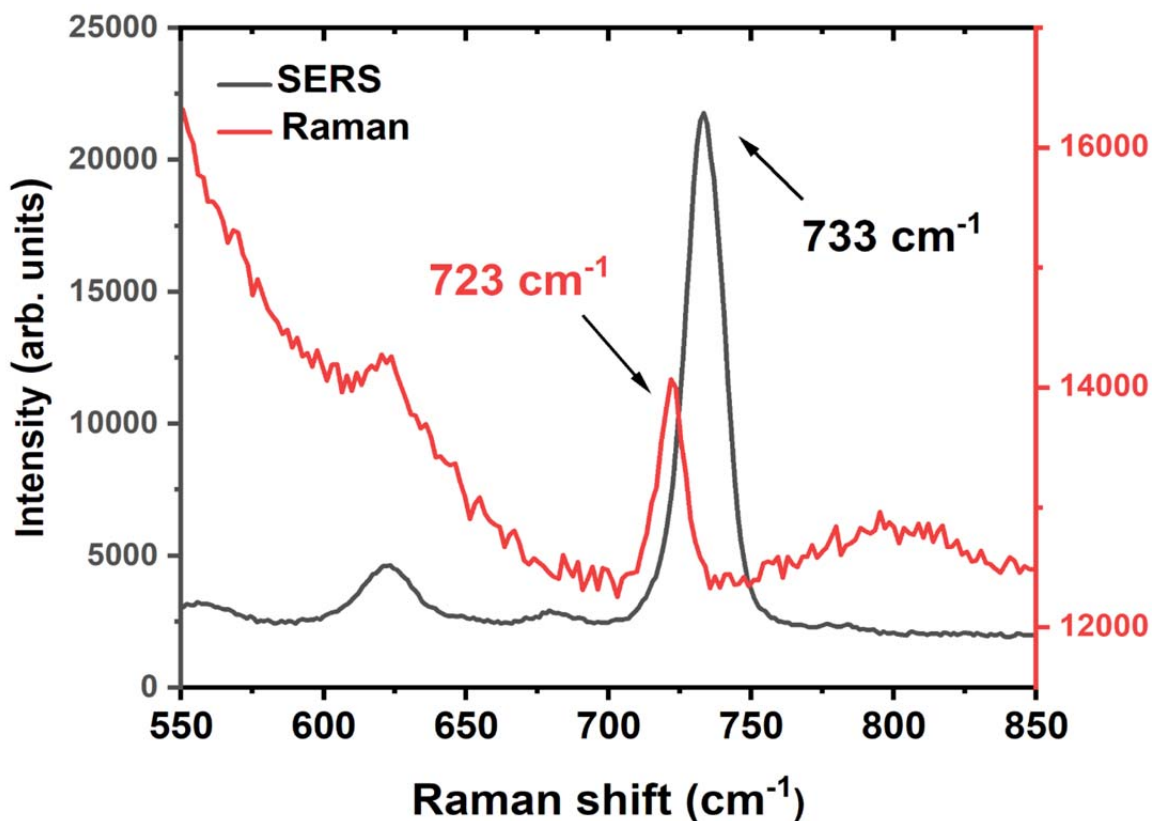


12

13 **Supplementary Figure 1. The scheme of a hyperspectral plasmon-enhanced stimulated**  
 14 **Raman scattering microscope.** Laser system: 80 MHz tunable femtosecond laser. AOM:  
 15 acousto-optic modulator. GM: 2D galvo mirror. PBS: polarizing beam splitter; QWP: quarter  
 16 wave plate; PD: photodiode. For spectral focusing, three or five rods were used in combined path  
 17 and one rod was used in Stokes path. In this way, the pump and Stokes pulses were chirped to  
 18 achieve a constant instantaneous frequency difference that drives a single Raman coherence. A  
 19 series of Raman shifts were generated by scanning the delay stage.

20

21 **Supplementary Figure**

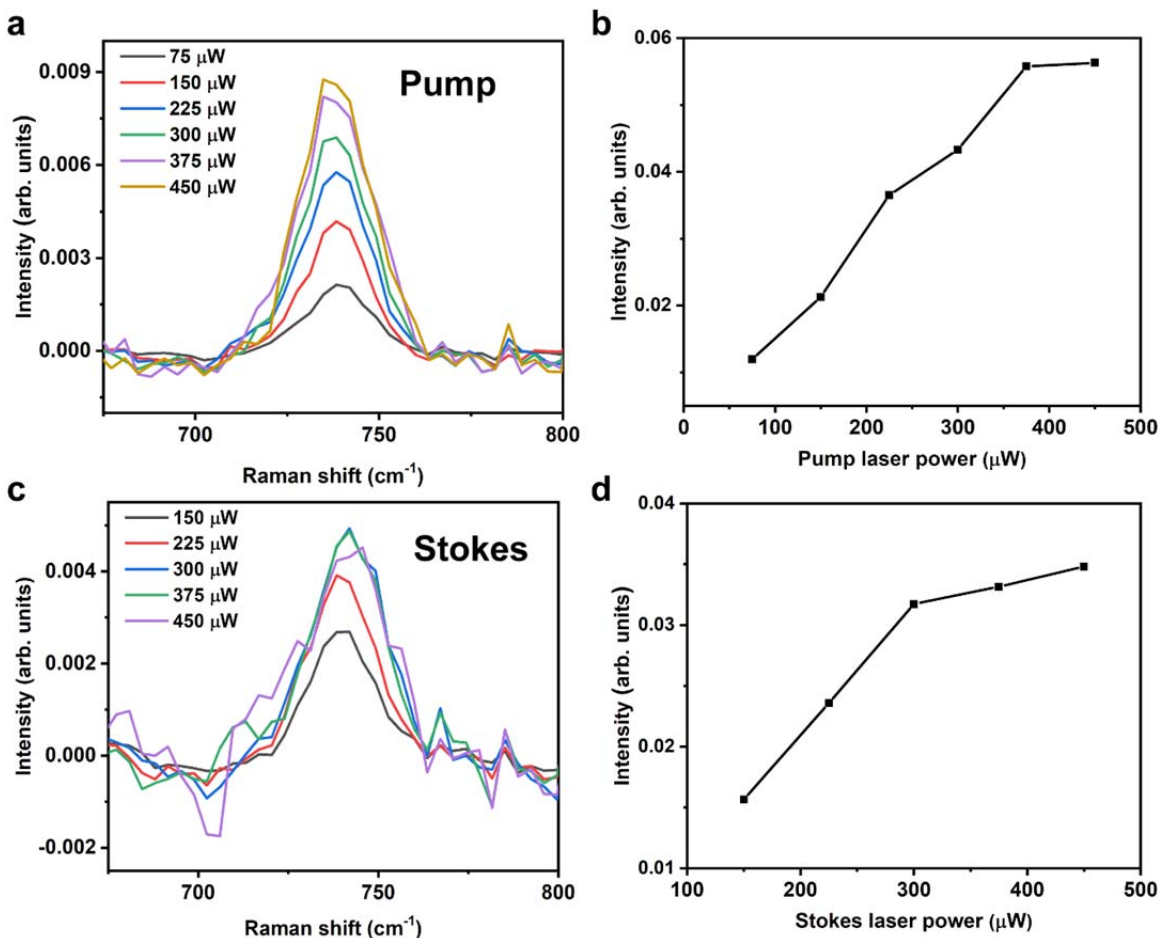


22

23 **Supplementary Figure 2. The SERS spectrum of adenine adsorbed on Au NPs aggregation**  
24 **substrate and the Raman spectrum of adenine solution.** The SERS spectrum (black) of  
25 adenine adsorbed on Au NPs aggregation substrate (5 mM in solution) has a peak at 733 cm<sup>-1</sup>.  
26 The Raman spectrum (red) of 5 mM adenine solution has a peak at 723 cm<sup>-1</sup>. The SERS spectrum  
27 was recorded with 5 s integration time, with a 50× objective and a 0.5 mW laser power at 785 nm.  
28 The Raman spectrum was recorded with 30 s integration time, with a 40× objective and an 80  
29 mW laser power at 532 nm. This 10 cm<sup>-1</sup> blue shift is due to the formation of metal-adenine  
30 complex.<sup>1</sup>.

31

32 **Supplementary Figure**

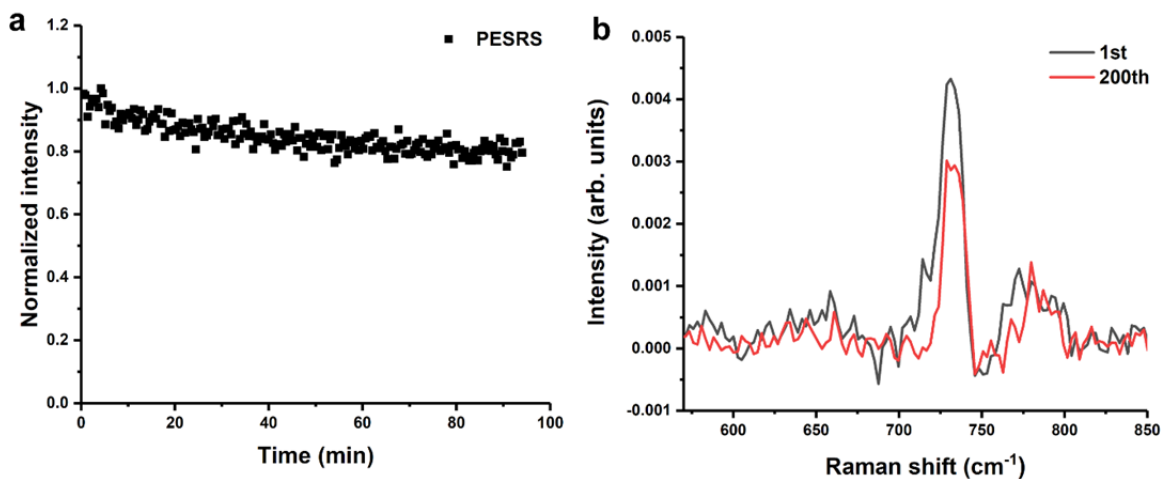


33

34 **Supplementary Figure 3. Dependence of plasmon-enhanced stimulated Raman scattering**  
 35 **(PESRS) signal on pump and Stokes laser power.** (a) The pump power dependent PESRS  
 36 spectra of adenine adsorbed on Au NPs aggregation substrate at the same position. The Stokes  
 37 power was kept at 150 μW. (b) The peak area at 733 cm<sup>-1</sup> of adenine obtained from (a) vs. pump  
 38 power. (c) The Stokes power dependent PESRS spectra of adenine adsorbed on Au NPs  
 39 aggregation substrate at the same position. The pump power was kept at 150 μW. (d) The peak  
 40 area at 733 cm<sup>-1</sup> of adenine obtained from (c) vs. Stokes power. The power value was the power  
 41 at the sample. The PESRS signal has a linear relationship with the pump and Stokes power under  
 42 a saturation power threshold (the sum of two laser power is c.a. 600 to 650 μW). The spectral  
 43 features are similar. All laser powers, used in whole PESRS experiments, were kept below this  
 44 threshold to minimize the photodamage of samples.

45

46 **Supplementary Figure**



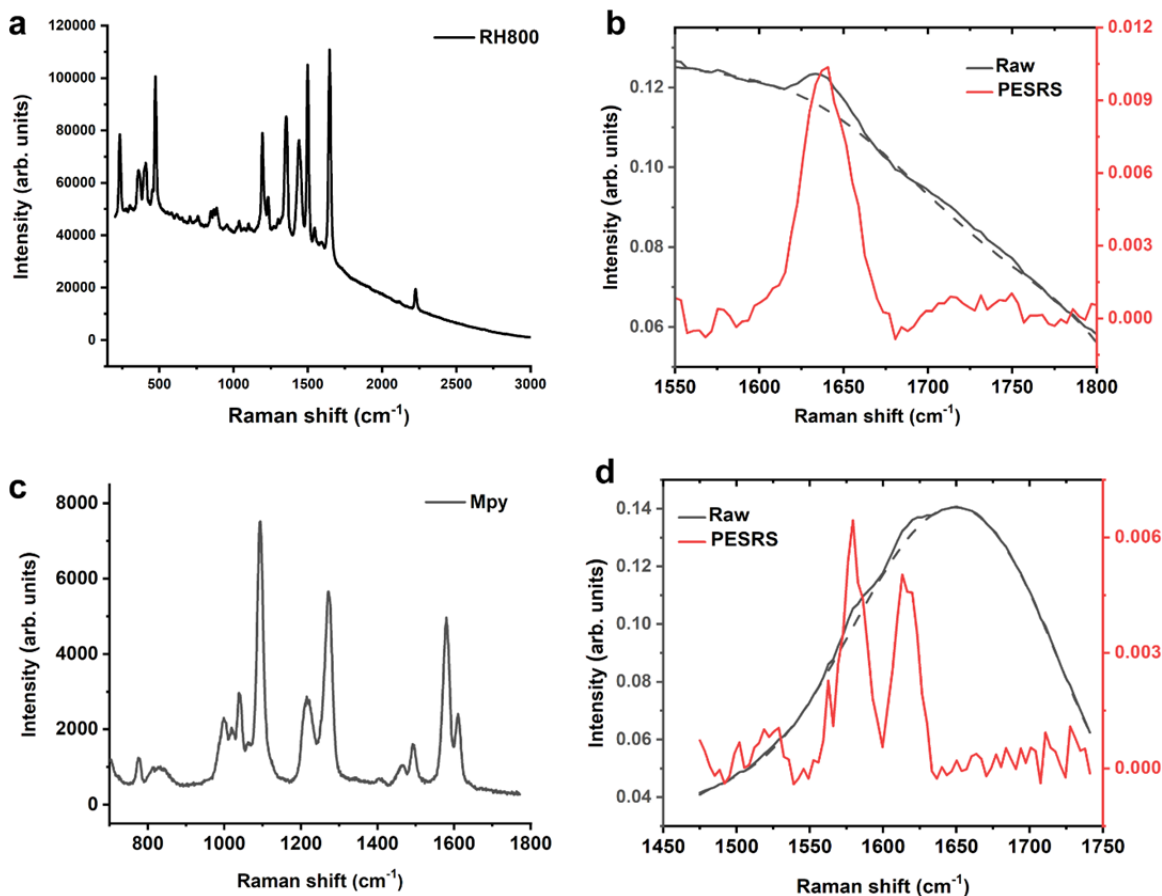
47

48 **Supplementary Figure 4. The photostability of PESRS signal in a 1.5 h continual exposure.**  
49 (a) The time-series of PESRS signal of adenine in 1.5 hour at the same location. About 20% of  
50 PESRS signal is lost in 1.5 h. (b) The 1<sup>st</sup> and 200<sup>th</sup> PESRS spectrum of adenine. 10  $\mu$ L of 1 mM  
51 adenine was dropped into centrifuged Au NPs and was dry in vacuum. The power of pump and  
52 Stokes was 0.15 mW. Image area: 30  $\mu$ m  $\times$  30  $\mu$ m with 300 nm step size. Pixel dwell time: 10  $\mu$ s.  
53 It took 0.47 min for one hyperspectral data. 200 hyperspectral data were continually obtained in  
54 94 min. Time-dependent hyperspectral data cubes were denoised via BM4D and subtracted  
55 background.

56

57

58 **Supplementary Figure**



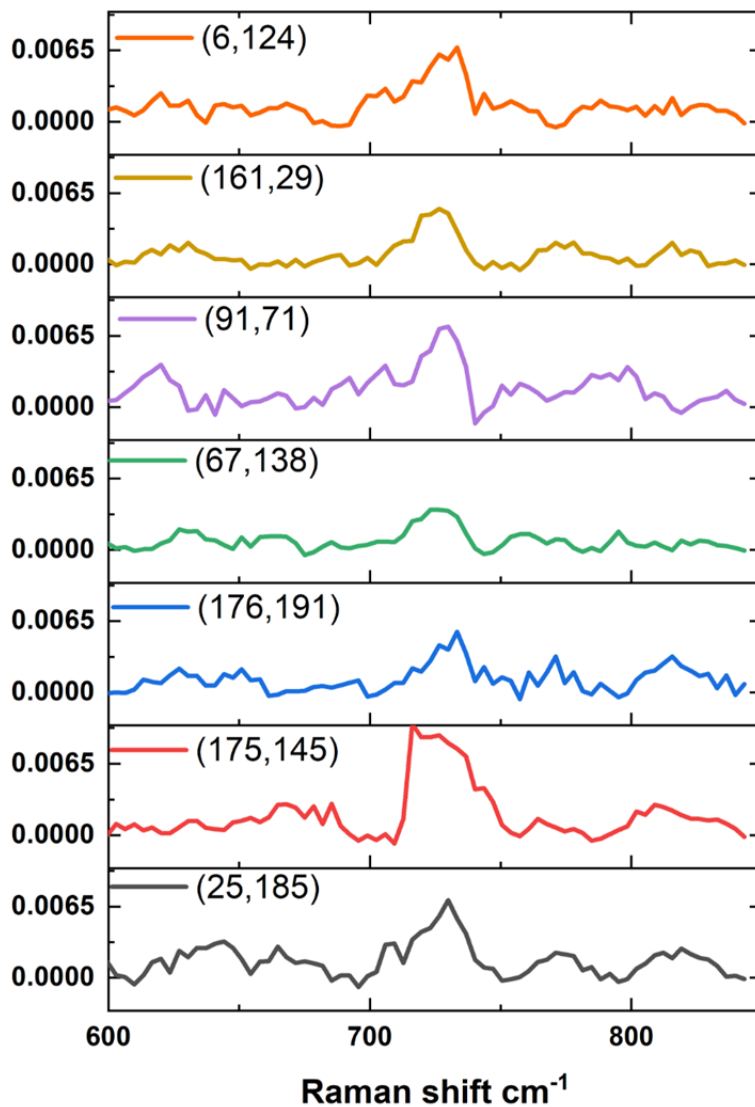
59

60 **Supplementary Figure 5. SERS and PESRS spectra of Rhodamine 800 (RH800) and 4-**  
 61 **mercaptopyridine (Mpy).** (a) The SERS spectrum of RH800 adsorbed on Au NPs. The spectrum  
 62 was recorded with 10 s integration time with a 50× objective and a 3 μW laser power at 785 nm.  
 63 (b) Original PESRS spectrum (black solid) and fitted background (black dash) of RH800  
 64 adsorbed on Au NPs. The background-subtracted PESRS spectrum (red) of RH800. 75 μW pump  
 65 laser (888 nm) and 50 μW Stokes laser were used. 10 μL of 85 μM RH800 was dropped into  
 66 centrifuged Au NPs sol and was dry in vacuum. (c) The SERS spectrum of Mpy adsorbed on Au  
 67 NPs. The spectrum was recorded with 2 s integration time with a 50× objective and a 300 μW  
 68 laser power at 785 nm. (d) Original PESRS spectrum (black solid) and fitted background (black  
 69 dash) of Mpy adsorbed on Au NPs. The background-subtracted PESRS spectrum (red) of Mpy.  
 70 150 μW pump laser (891 nm) and 150 μW Stokes laser were used. 10 μL of 5.7 mM Mpy was  
 71 dropped into centrifuged Au NPs sol and was dry in vacuum. This result indicated that our  
 72 method can obtain PESRS spectra from a variety of molecules.

73

74

75 **Supplementary Figure**



76

77 **Supplementary Figure 6. Representative single-pixel PESRS spectra of adenine from a**  
78 **single image indicate good reproducibility.** Representative single-pixel PESRS spectra of  
79 adenine, obtained from aggregated Au NPs substrate (the same hyperspectral data cube in Figure  
80 2). The labels of each spectrum indicate the X-Y pixel coordinate.

81

82 **Supplementary Note 1. The estimation of local enhancement factor of PESRS.**

83 In stimulated Raman scattering, the signal intensity is calculated as<sup>2</sup>:

$$I = N \times \sigma \times P \times S$$

84 Where,  $I$  is the intensity,  $N$  is the number of molecules under the laser spot,  $\sigma$  is the molecular

85 Raman scattering cross-section.  $P$  is the pump laser power.  $S$  is the Stokes laser power.

86 Enhancement factor (EF) of PESRS relative to normal SRS is defined as a ratio of PESRS over

87 SRS cross-sections ( $EF = \sigma_{PESRS}/\sigma_{SRS}$ ). To estimate the EF of PESRS, we calculated the power-

88 and concentration- averaged intensity between PESRS and SRS as following:

$$\sigma_{PESRS} = \frac{I_{PESRS}}{N_{PESRS} \times P_{PESRS} \times S_{PESRS}}$$
$$\sigma_{SRS} = \frac{I_{SRS}}{N_{SRS} \times P_{SRS} \times S_{SRS}}$$

89 Thus ,

$$EF = \frac{\sigma_{PESRS}}{\sigma_{SRS}} = \frac{I_{PESRS}}{I_{SRS}} \times \frac{N_{SRS}}{N_{PESRS}} \times \frac{P_{SRS}}{P_{PESRS}} \times \frac{S_{SRS}}{S_{PESRS}}$$

90 As shown in **Supplementary Figure 7**, the SRS spectrum (average  $200 \times 200$  pixel area spectra)

91 of 5 mM adenine solution was measured at the power of 15 mW (Pump) and 100 mW (Stokes)

92 and the PESRS spectrum (average  $3 \times 3$  pixel area spectra) of adsorbed adenine was measured at

93 the power of 0.5 mW (Pump) and 0.5 mW (Stokes). We assumed the size of the laser spot was

94 500 nm, the size of adenine was  $0.5 \text{ nm}^2$  per molecule. Au NPs was a monolayer under the laser

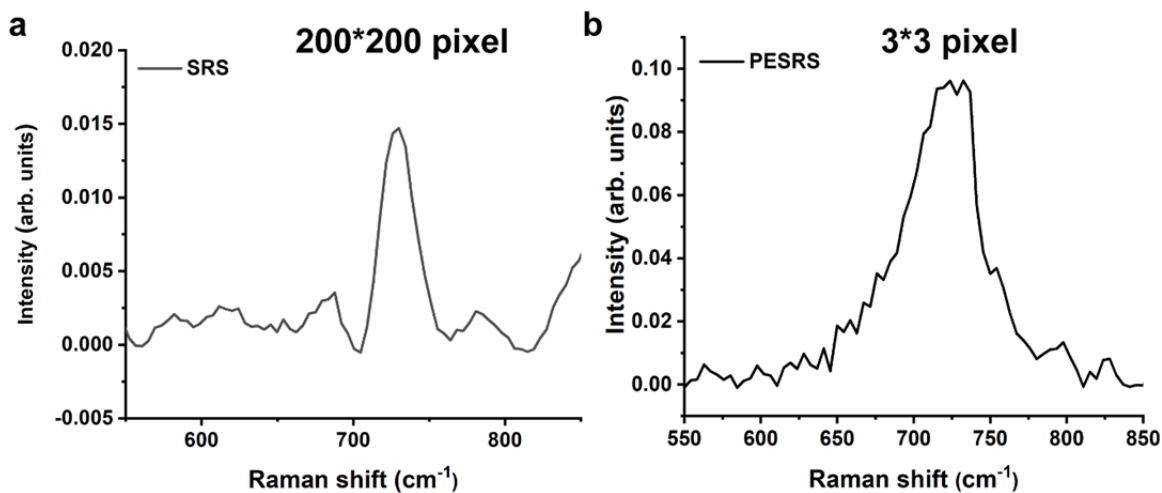
95 spot and a monolayer adenine adsorbed on Au NPs surface. The number of molecules in detection

96 volume (c.a.  $30 \mu\text{m} \times 30 \mu\text{m} \times 1 \mu\text{m} = 900 \mu\text{m}^3$ ) was about  $2.7 \times 10^9$  for SRS detection. The

97 number of molecules on the surface can be estimated as about  $1.6 \times 10^6$  for PESRS. In this way,

98 the local enhancement factor of PESRS was about  $7 \times 10^7$ .

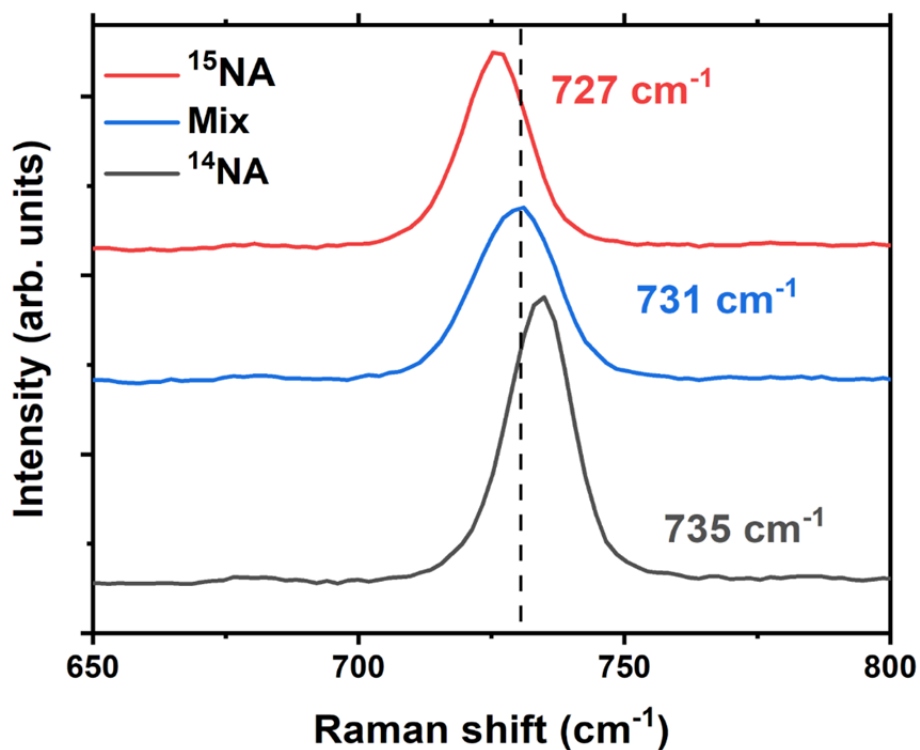




99

100 **Supplementary Figure 7. PESRS and SRS spectra of adenine.** (a) The SRS spectrum of 5 mM  
 101 adenine solution (average 200×200 pixel area spectra). Pump power: 15mW, Stokes power: 100  
 102 mW. (b) The PESRS spectrum of adsorbed adenine on Au NPs-SiO<sub>2</sub> substrate (average 3×3 pixel  
 103 area spectra). Pump power: 0.5 mW, Stokes power: 0.5 mW.

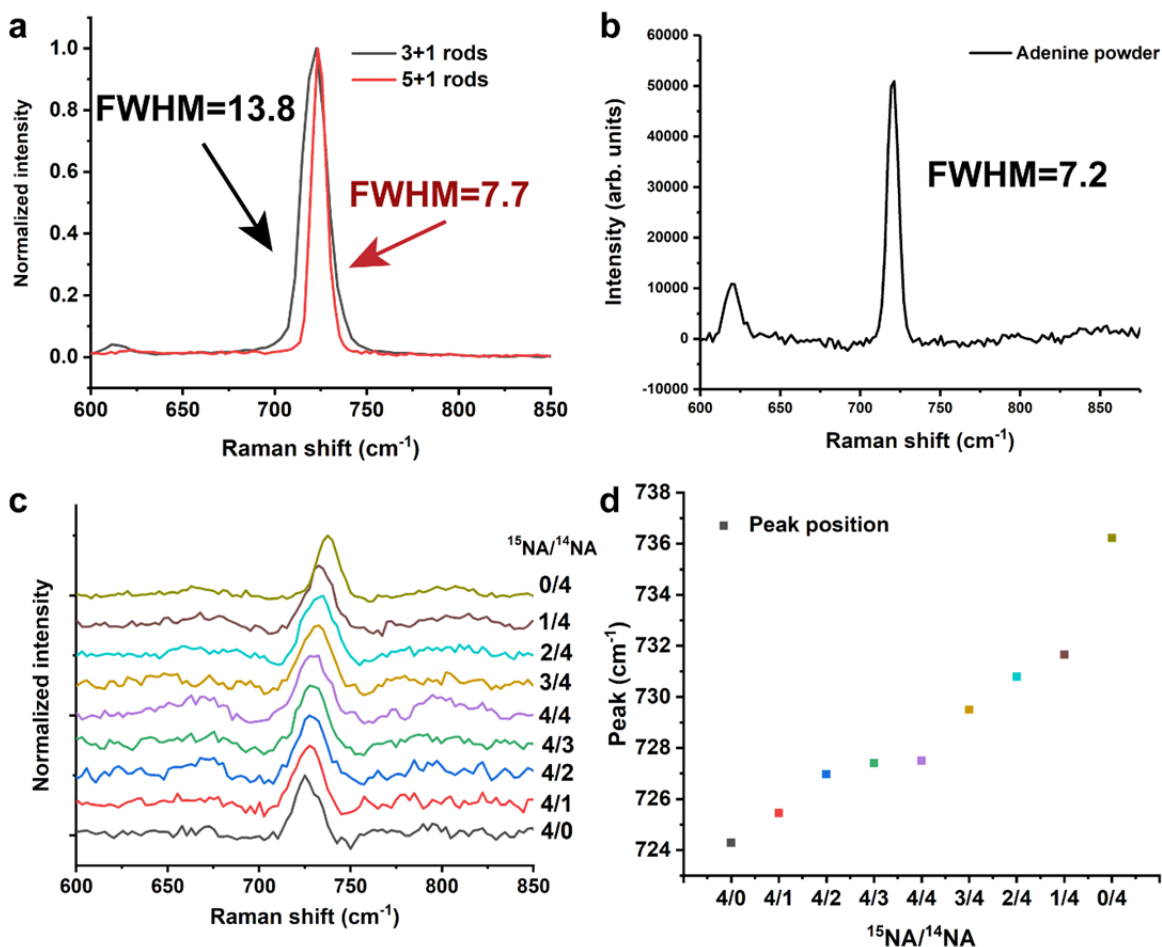
104



106

107 **Supplementary Figure 8. The SERS spectra of pure  $^{14}\text{NA}$ , pure  $^{15}\text{NA}$  and their equimolar**  
108 **mixture adsorbed on Au NPs aggregation substrates.** The SERS spectra of pure  $^{14}\text{NA}$ , pure  
109  $^{15}\text{NA}$  and their equimolar mixture adsorbed on Au NPs aggregation substrates (1 mM in solution).  
110 The pure  $^{14}\text{NA}$  SERS spectrum has a peak at 735  $\text{cm}^{-1}$ , the pure  $^{15}\text{NA}$  SERS spectrum has a peak  
111 at 727  $\text{cm}^{-1}$ , and the equimolar mixture SERS spectrum has a peak at 731  $\text{cm}^{-1}$ . These single  
112 isotope SERS spectra match well with the corresponding PESRS spectra.

113

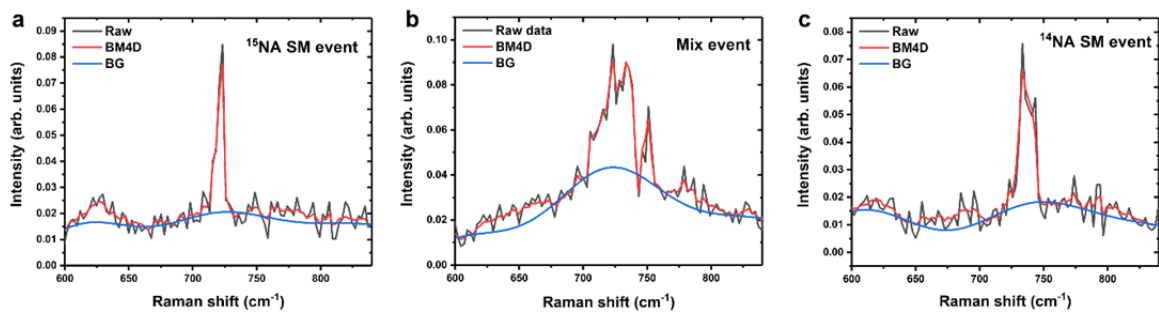


115  
 116 **Supplementary Figure 9. Spectral resolution of spectral focusing SRS microscopy.** (a) The  
 117 SRS spectra and corresponding FWHM of adenine powder measured by different chirped laser.  
 118 3+1 rods: 3 rods in combined light path and 1 rod in Stokes light path. 5+1 rods: 5 rods in  
 119 combined light path and 1 rod in Stokes light path. (b) The spontaneous Raman spectrum of  
 120 adenine powder measured by Renishaw inVia Raman microscope with 1200/mm grating. Laser:  
 121 633 nm. (c) PESRS spectra as a function of concentration ratio of  $^{15}\text{NA}$  and  $^{14}\text{NA}$ . (d) PESRS  
 122 peak positions of mixture samples as a function of concentration ratio of  $^{15}\text{NA}$  and  $^{14}\text{NA}$ . With  
 123 the increasing of  $^{14}\text{NA}$ , the PESRS peaks of mixture shift to high wavenumber. The PESRS  
 124 spectra were measured by 5+1 rods. This result indicates that with a spectral resolution of  $7\text{ cm}^{-1}$ ,  
 125 our PESRS microscope is able to distinguish the concentration ratio of  $^{15}\text{NA}$  and  $^{14}\text{NA}$ .

126

127

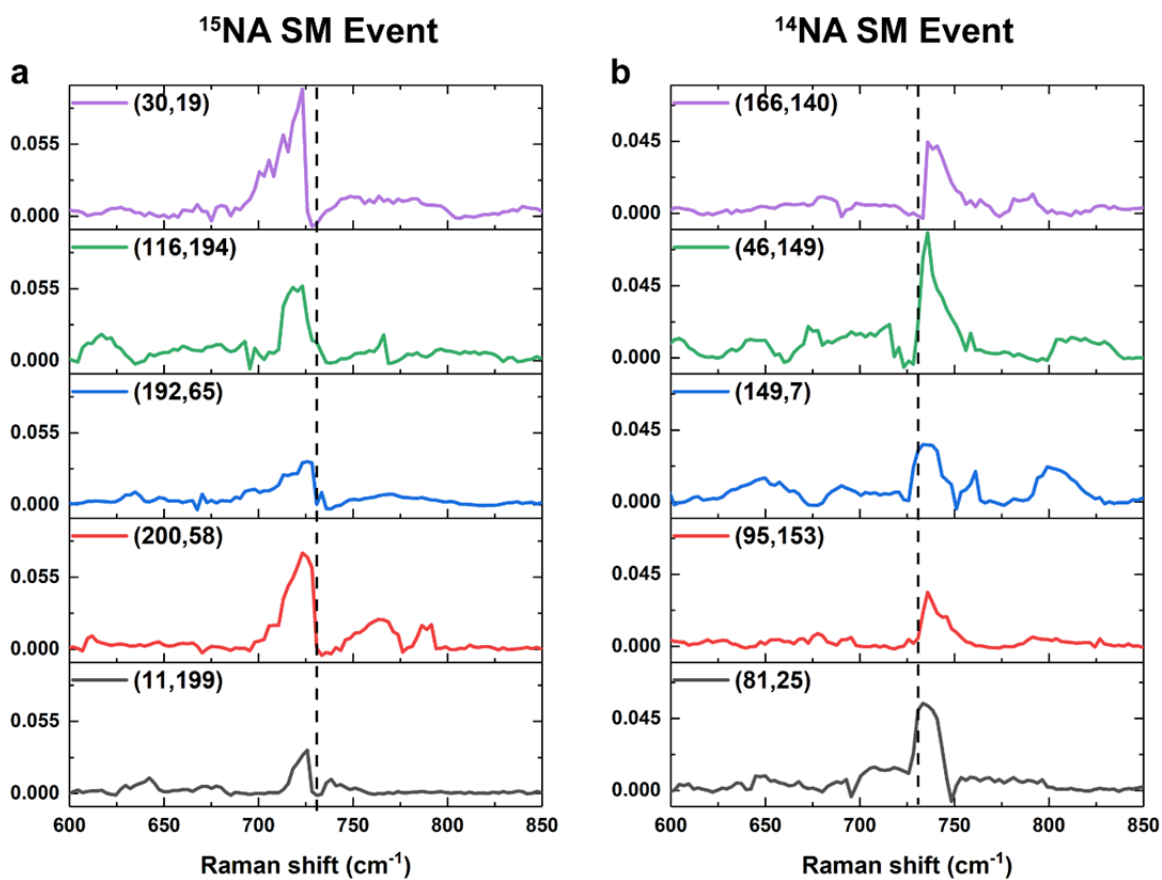
128 **Supplementary Figure**



129

130 **Supplementary Figure 10. The corresponding single molecule spectra with and without**  
131 **denoising and fitting background.** The corresponding single-pixel PESRS spectra of <sup>15</sup>NA  
132 single molecule event (a), mix event (b), and <sup>14</sup>NA single molecule event (c) without denoising,  
133 after denoising and fitting background in Figure 4b.

134



136

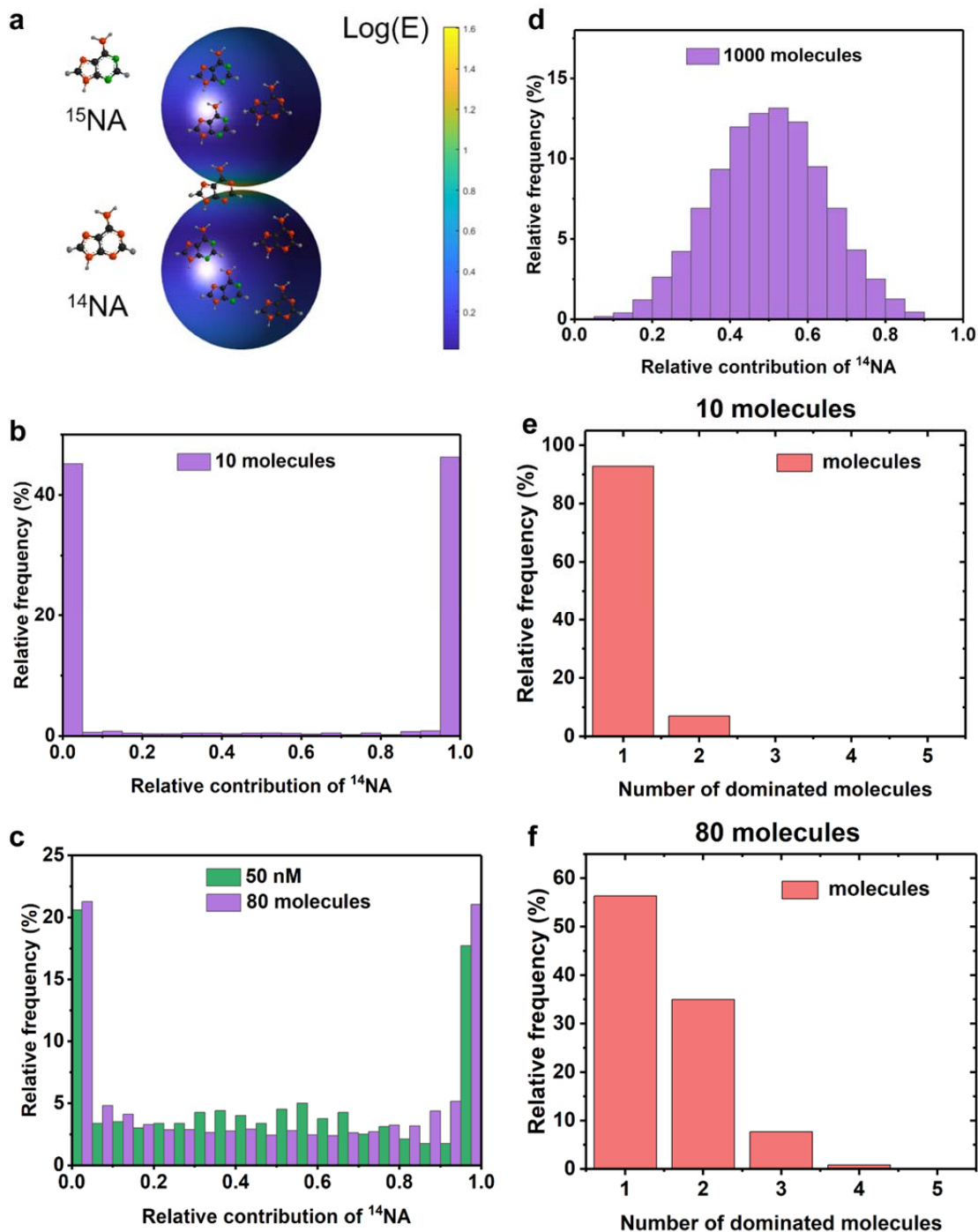
137 **Supplementary Figure 11. The representative single-molecule events of adenine in a PESRS**  
138 **image.** The representative single-molecule (SM) events from 50 nM adenine sample. Left column:  
139 pure  $^{15}\text{NA}$  single-molecule events, Right column: pure  $^{14}\text{NA}$  single-molecule events. The vertical  
140 dash lines indicate the position of  $730\text{ cm}^{-1}$ . Legends indicate the X-Y coordinate in PESRS image.

141

## 142 **Supplementary Note 2. The simulated single-molecule PESRS data**

143 Here, we introduced a model example to describe the statistics of single-molecule PESRS  
144 signal in a hot spot. This model was based on the previous bianalyte approach mode developed by  
145 Eric Le Ru, PG Etchegoin, et al.<sup>3</sup> First, we used the boundary element method approach<sup>4-6</sup> to  
146 calculate a local electric field distribution on a representative hot spot. Supplementary Figure 12a  
147 presented the simulated local electric field distribution of the representative hot spot (a dimer  
148 formed by two 60 Au NPs with a 1 nm gap). Then, we assumed that we had a certain number of  
149 molecules of two isotopic adenines ( $N_{14}$  and  $N_{15}$ ) on the hot spot. We generated random locations  
150 of molecules in the hot spot and every molecule felt a corresponding local electric field in the hot  
151 spot.<sup>7</sup> Then, we calculated the total intensity produced by each type of molecules ( $I_{14}$  and  $I_{15}$ ) by  
152 summing over the corresponding intensity of every molecules. Because the Raman cross section  
153 of  $^{14}\text{NA}$  and  $^{15}\text{NA}$  were the same, the ratio of  $I_{14}/(I_{14}+I_{15})$  was also the ratio of the average number  
154 of  $^{14}\text{NA}$  contributing to the signal. We repeated this process for many times (as a large number of  
155 events). In order to mimic experiment condition, we only counted the events above a threshold  
156 (0.2 % of maximum total intensity) and obtained the histogram for relative contribution of  $^{14}\text{NA}$ .  
157 In addition, we analyzed the number of signal-dominated molecules, which contribute 80 % of  
158 total signal, in every single molecule events (ratio  $\approx 0$  and  $\approx 1$ ). **Supplementary Figure 12** shows  
159 the the simulated results for repeating 100000 events with  $N_{14}=N_{15}=10$  (b), 80 (c), and 1000 (d)  
160 molecules, respectively. For  $N_{14}=N_{15}=10$ , as shown in **Supplementary Figure 12b**, events were  
161 dominant by the ratio  $\approx 0$  and  $\approx 1$ . **Supplementary Figure 12e** indicates that 90 % single  
162 molecule events (the ratio  $\approx 0$  and  $\approx 1$ ) was mainly contributed by 1 molecule for 10 molecules  
163 simulation. As shown in **Supplementary Figure 12c**, for  $N_{14}=N_{15}=80$ , inevitably, there were  
164 more mixed-signal events than that in  $N_{14}=N_{15}=10$ . However, **Supplementary Figure 12f** clearly  
165 indicates that 55 % single molecules events were mainly contributed by 1 molecule. This result  
166 indicated that the single molecule events in 80 molecules simulation can be attributed to real  
167 single-molecule events with a high probability. The many-molecules regime,  $N_{14}=N_{15}=1000$ . The

168 histogram (**Supplementary Figure 12d**) looks like a Gaussian distribution centered at the  
169 ratio=0.5. Most of events have contributions from many molecules. As shown in **Supplementary**  
170 **Figure 12c**, our 50 nM experimental result (green) matched well the simulated result (purple) of  
171 80 molecules. This result indicated that our experiment has achieved a single-molecules detection  
172 regime.



173

174 **Supplementary Figure 12. The simulated single-molecule PESRS data** (a) The local electric  
 175 field distribution of the hot spot. The hot spot was formed by two 60 nm Au NPs with a 1 nm gap.  
 176 Each molecule adsorbed on a certain location can experience a corresponding local electric field.  
 177 (b & d) The histograms (purple) of the relative contribution of  $^{14}\text{NA}$  in the simulated results with  
 178  $N_{14}=N_{15}=10$  (b), 1000 (d) molecules, respectively. (c) The histograms of the relative contribution  
 179 of  $^{14}\text{NA}$  in the 50 nM mixture sample (green) and simulated result (purple) of  $N_{14}=N_{15}=80$ . (e-f)  
 180 The histogram of number of dominated molecules which contribute 80 % total signal in single  
 181 molecule events with  $N_{14}=N_{15}=10$  (e), 80 (f).



182

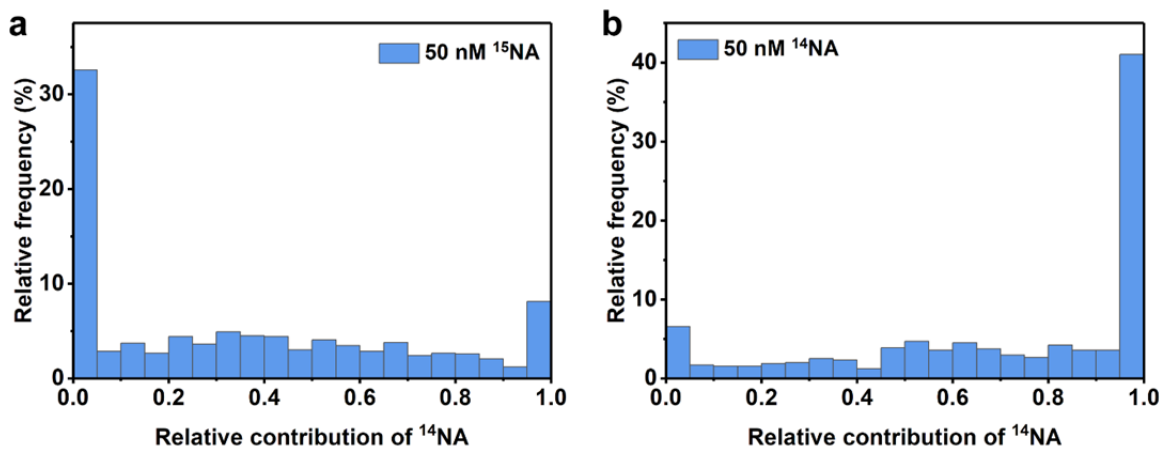
183 As a control experiment, we measured 50 nM pure  $^{14}\text{NA}$  and pure  $^{15}\text{NA}$  samples, respectively.

184 **Supplementary Figure. 13a&b** shows the histograms of relative contribution of  $^{14}\text{NA}$  of isotopic

185 pure  $^{14}\text{NA}$  and pure  $^{15}\text{NA}$  samples. The histogram of pure  $^{14}\text{NA}$  and pure  $^{15}\text{NA}$  sample dominated

186 by the ratio  $\approx 1$  (**Supplementary Figure 13b**) and  $\approx 0$  (**Supplementary Figure 13a**),

187 respectively.



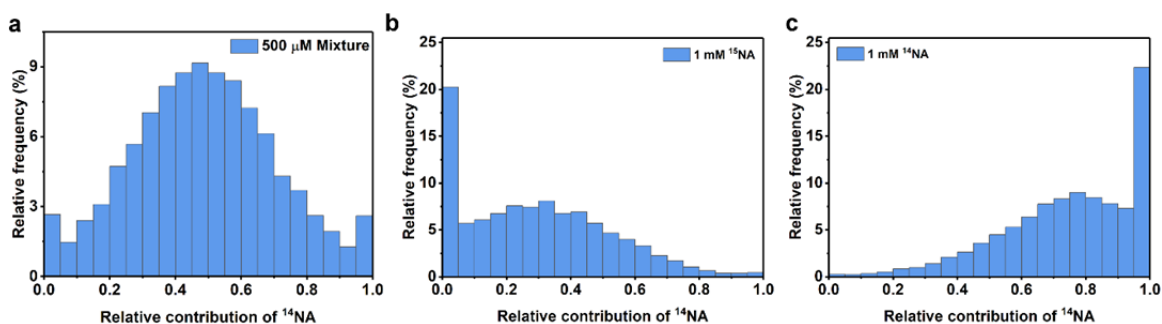
188

189 **Supplementary Figure 13. The histograms of the relative contribution of  $^{14}\text{NA}$  in pure**  
190 **sample.** The histograms of the relative contribution of  $^{14}\text{NA}$  in (a) the 50 nM  $^{15}\text{NA}$  sample and (b)  
191 50 nM  $^{14}\text{NA}$  sample.

192

193 **Supplementary Note 3. The reliability of multivariate curve resolution (MCR) analysis for**  
194 **Fano-shape spectra**

195 To verify the reliability of multivariate curve resolution (MCR) analysis for Fano-shape spectra,  
196 we measured a 1 mM pure  $^{14}\text{NA}$ , a pure  $^{15}\text{NA}$  and their mixture sample. As we expected, the  
197 histogram of the relative contribution of  $^{14}\text{NA}$  in 500  $\mu\text{M}$  of mixture sample (**Supplementary**  
198 **Figure 14a**) looks like a Gaussian distribution center at the ratio=0.5. In addition, the histogram  
199 of 1 mM pure  $^{14}\text{NA}$  sample was dominated by pure  $^{14}\text{NA}$  signal (ratio  $\approx 1$ ), as show in  
200 **Supplementary Figure 14c**. While “mixture” signals also were observed in the histogram which  
201 might result from the various dispersive line shape of PESRS in different single-pixel spectra.  
202 Those various dispersive line shape depended on the local LSPR frequency and local  
203 enhancement. Similarly, in the pure  $^{15}\text{NA}$  sample (**Supplementary Figure 14b**), a significant  
204 portion of signals was assigned to pure  $^{15}\text{NA}$  (ratio  $\approx 0$ ) and little to  $^{14}\text{NA}$ .



206 **Supplementary Figure 14. The histograms of the relative contribution of  $^{14}\text{NA}$  in ensemble**  
207 **pure and mixed sample.** The histograms of the relative contribution of  $^{14}\text{NA}$  in 500  $\mu\text{M}$  the  
208 mixture of  $^{14}\text{NA}$  and  $^{15}\text{NA}$  sample (a), 1 mM  $^{15}\text{NA}$  sample (b) and 1 mM  $^{14}\text{NA}$  sample (c).

209

210 In addition, we used the Fano-line shape function ( $f(x) = A \left\{ \frac{(q + \frac{x-x_0}{\Gamma/2})^2}{1 + (\frac{x-x_0}{\Gamma/2})^2} \right\}$ ) to fit the single pixel

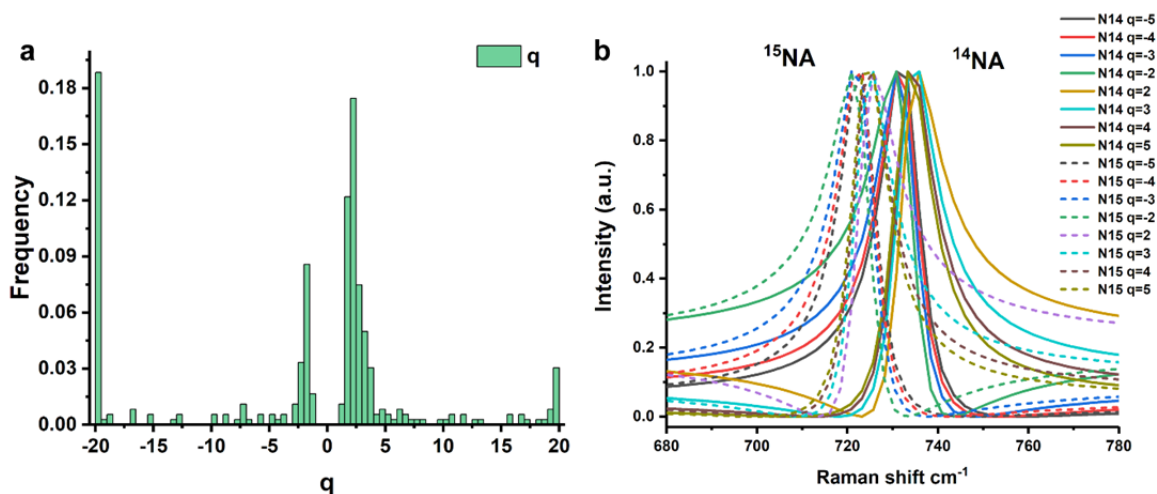
211 spectra of the 50 nM adenine sample. Here,  $A$  is the amplitude of each peak,  $q$  is the Fano

212 asymmetry parameter,  $x_0$  is the center frequency of vibrational feature,  $x$  is the Raman shift,  $\Gamma$  is

213 the line width. We find that most of fitted Fano asymmetry parameter ( $q$ ) are larger than 2 or

214 smaller than -2 (**Supplementary Figure 15a**). Based on this result, we simulated a series of  $q$

215 value dependent  $^{14}\text{NA}$  and  $^{15}\text{NA}$  spectra as shown in **Supplementary Figure 15b**. The simulation  
 216 result show that when  $q > 2$  or  $< -2$ , the different  $q$  value can induce the shift of peak position.  
 217 While,  $^{14}\text{NA}$  and  $^{15}\text{NA}$  spectra still can be differentiated. Our results indicated that various  
 218 dispersive line shapes of PESRS spectra slightly affect the Raman peak frequency. However, this  
 219 slight frequency shift has no obvious impact on the molecular assignment between  $^{14}\text{NA}$  and  
 220  $^{15}\text{NA}$ .

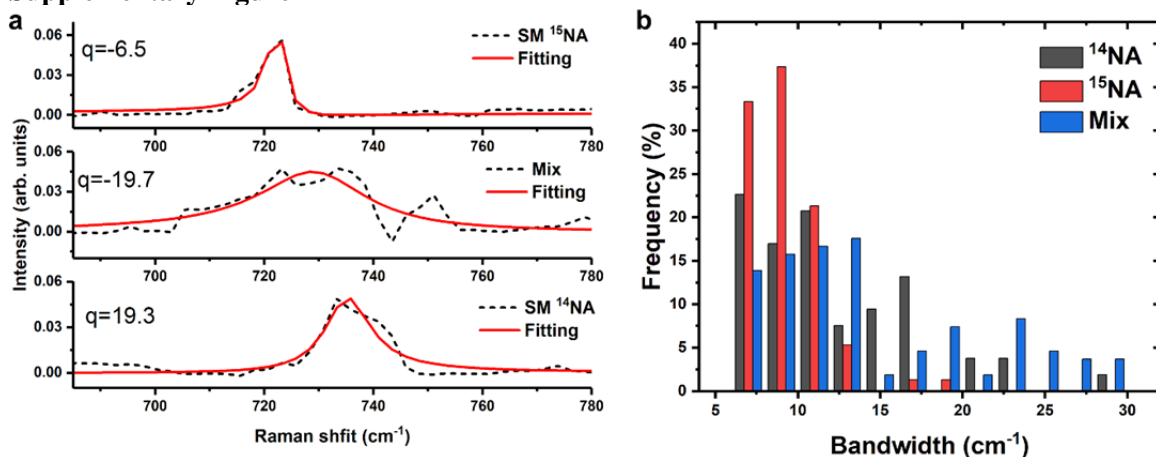


221

222 **Supplementary Figure 15. Fano-line fitting and simulation spectra** (a) The distribution of  $q$   
 223 value of PESRS spectra of 50 nM adenine. (b) Simulation  $^{14}\text{NA}$  and  $^{15}\text{NA}$  spectra with a function  
 224 of Fano  $q$  parameter. Position:  $x_0=733\text{ cm}^{-1}$  and  $726\text{ cm}^{-1}$  for  $^{14}\text{NA}$  and  $^{15}\text{NA}$ , respectively. Width:  
 225  $\Gamma=10\text{ cm}^{-1}$ .

226

227 **Supplementary Figure**



228

229 **Supplementary Figure 16. Bandwidth statistics in a PESRS image.** (a) The representative  
 230 single-pixel PESRS spectra (dash lines) of <sup>15</sup>NA single molecule event, mix event, and <sup>14</sup>NA  
 231 single molecule event fitted with a Fano-lineshape function (red lines). The fitting function was

232 shown as following:  $f(x) = A \left\{ \frac{\left( q + \frac{x-x_0}{\Gamma/2} \right)^2}{1 + \left( \frac{x-x_0}{\Gamma/2} \right)^2} \right\}$ . Here,  $A$  is the amplitude of each peak,  $q$  is the Fano

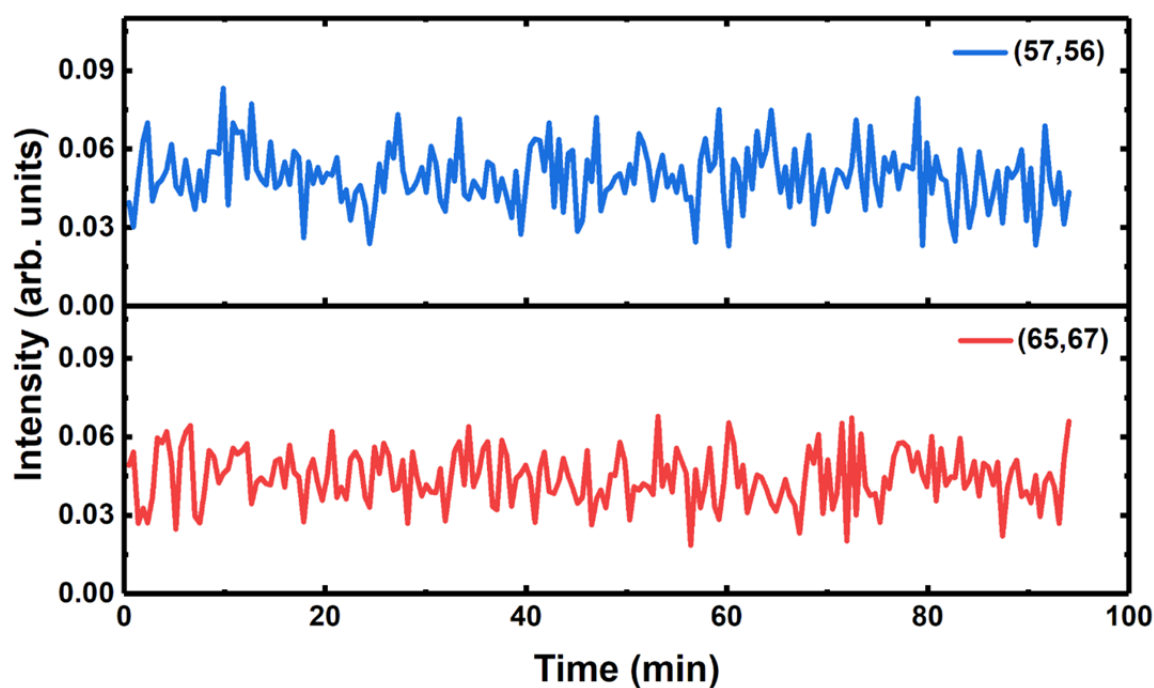
233 asymmetry parameter,  $x_0$  is the center frequency of vibrational feature,  $\Gamma$  is the line width.  
 234 Corresponding fitted  $q$  value indicated in text. (b) Histogram displaying the width of the peak  
 235 bandwidth for SM <sup>14</sup>NA (black) events, SM <sup>15</sup>NA (red) events, and mix (blue) event. The  
 236 bandwidth of mixed events (blue, average:  $14.6 \pm 6.5 \text{ cm}^{-1}$ ) is larger than the bandwidths of single  
 237 molecule spectra (black and red, average:  $10.5 \pm 3.9 \text{ cm}^{-1}$ ).

238

239 **Supplementary Note 4. The time-lapsed PESRS images collected on a 50 nM and 1 mM**  
240 **adenine sample**

241 To further validate the single-molecules sensitivity of PESRS, we measured the time-series  
242 PESRS signal (as shown in **Supplementary Movie 2**) from a 50 nM adenine solution adsorbed  
243 on Au NPs at the same location. 10  $\mu\text{L}$  of 50 nM adenine was dropped into centrifuged Au NPs  
244 and was dry in vacuum. The power of pump and Stokes was 0.15 mW. Image area: 30  $\mu\text{m}$   $\times$  30  
245  $\mu\text{m}$  with 300 nm step size. Pixel dwell time: 10  $\mu\text{s}$ . It took 0.47 min for one hyperspectral data.  
246 200 hyperspectral data were continually obtained in 94 min. Movie S2 shows the BM4D denoised  
247 and background-corrected PESRS signal. Previous time-series PESRS of 1 mM adenine (as  
248 shown in **Supplementary Movie 1**) was used as a control experiment.

249 As shown in Fig 4, representative time traces of 50 nM adenine (**Fig 4e**) show that strong  
250 Raman signal fluctuations during the PESRS measurements at the same locations. While, 1 mM  
251 adenine ensemble sample results (**Supplementary Figure 17**) show a stable intensity change.  
252 This spectral blinking phenomenon is consider an additional signature of the behavior of single  
253 molecule spectral sensitivity. In addition, **Fig 4e** shows representative photodamage processes of  
254 50 nM adenine. The 50 nM sample exhibited a single-step photodamage process, while the  
255 ensemble molecule sample (1 mM) result shows a stable intensity trace (**Supplementary Figure**  
256 **17**). Our time-series PESRS results exhibited characteristic single-molecules behaviors including  
257 blinking and single-step photodamage, which further verify the single-molecules sensitivity of  
258 PESRS.

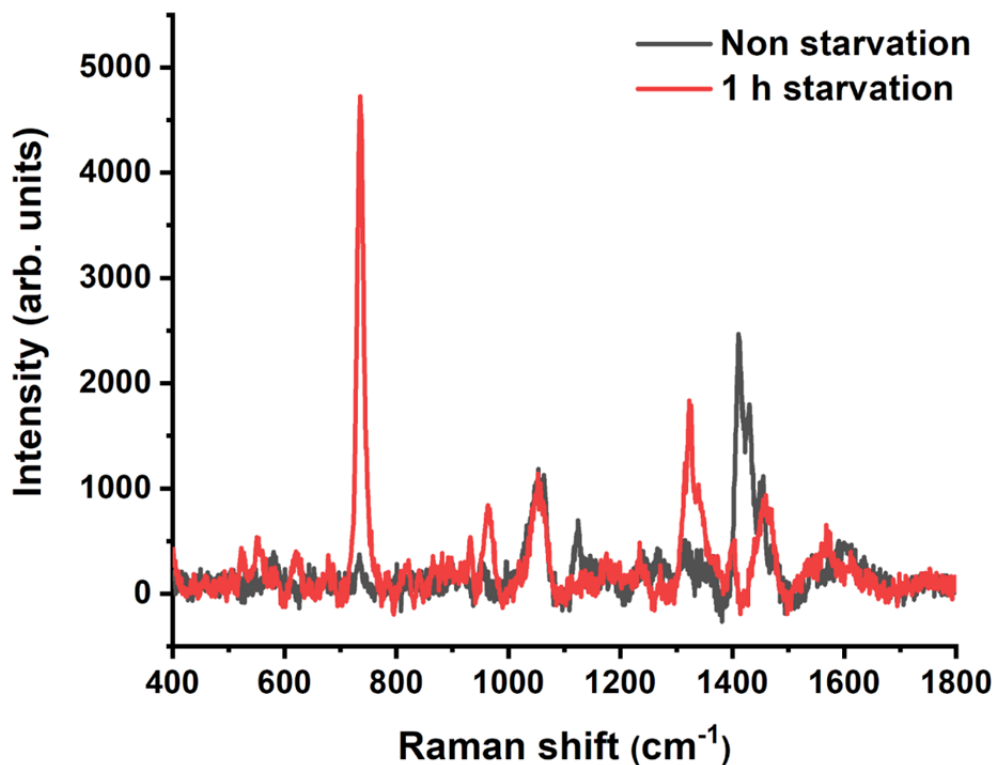


259

260 **Supplementary Figure 17. The time-lapsed PESRS images.** Representative time traces of  
261 PESRS spectra collected of 1 mM adenine solution showing relative stable intensity traces. The  
262 inside labels show the the X-Y coordinate where the spectra were recorded

263

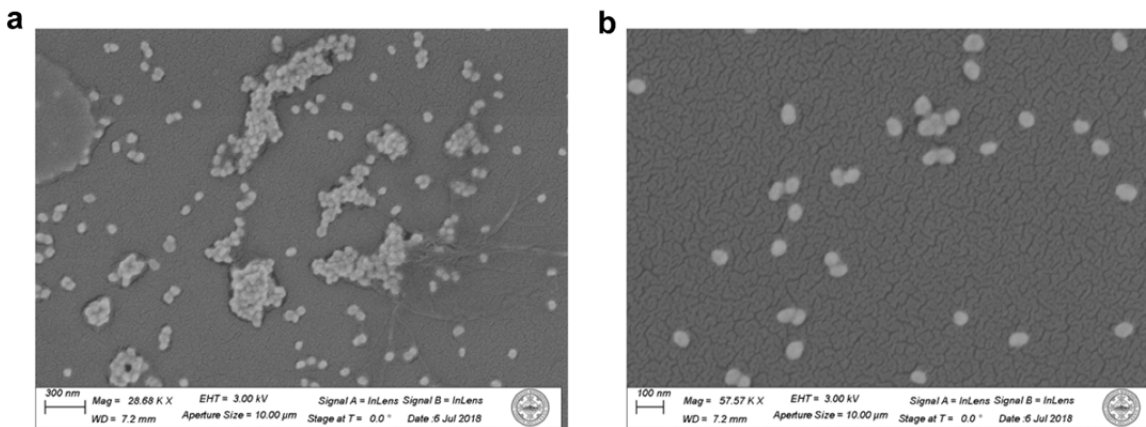
264



265

266 **Supplementary Figure 18. SERS spectra of starved *S. aureus* and non-starved *S. aureus*.**  
267 SERS spectra of starved *S. aureus* (red) and non-starved *S. aureus* (black). After 1 hour starvation  
268 in pure water, the SERS spectrum of *S. aureus* closely resembled the SERS of adenine. This  
269 result indicates that the adenine appeared at the outer layer of *S. aureus* and in the extracellular  
270 metabolome as resulting from the bacterial cell stress response to the no-nutrient, water-only  
271 environment. The spectra were recorded with 10 s integration time with a 20× objective and a 0.5  
272 mW laser power at 785 nm.

273



274

275 **Supplementary Figure 19. SEM images of Au NPs colloid.** The scale bar in (a) is 300 nm, and  
 276 in (b) is 100 nm. The size of Au NPs is around 50 to 60 nm.

277

278

279

280

## 281 **Supplementary References**

- 282 1. Xiao, Y.-J., Chen, Y.-F. & Gao, X.-X. Comparative study of the surface enhanced near  
 283 infrared Raman spectra of adenine and NAD<sup>+</sup> on a gold electrode. *Spectrochim. Acta A*  
 284 **55**, 1209-1218 (1999).
- 285 2. Cheng, J.-X. & Xie, X.S. Coherent Raman scattering microscopy. (CRC press, Boca  
 286 Raton; 2016).
- 287 3. Etchegoin, P.G., Meyer, M., Blackie, E. & Le Ru, E.C. Statistics of single-molecule  
 288 surface enhanced Raman scattering signals: Fluctuation analysis with multiple analyte  
 289 techniques. *Anal. Chem.* **79**, 8411-8415 (2007).
- 290 4. De Abajo, F.G. & Howie, A. Retarded field calculation of electron energy loss in  
 291 inhomogeneous dielectrics. *Phys. Rev. B* **65**, 115418 (2002).
- 292 5. De Abajo, F.G. Optical excitations in electron microscopy. *Rev. Mod. Phys.* **82**, 209  
 293 (2010).
- 294 6. Hohenester, U. & Trugler, A. Interaction of single molecules with metallic nanoparticles.  
 295 *IEEE J. Sel. Top. Quantum Electron.* **14**, 1430-1440 (2008).
- 296 7. Prince, R.C., Frontiera, R.R. & Potma, E.O. Stimulated Raman scattering: from bulk to  
 297 nano. *Chem. Rev.* **117**, 5070-5094 (2016).

298